Enhanced ferromagnetism and ferroelectricity in multiferroic $CuCr_{1-x}Ni_xO_2$

Shijun Luo, K. F. Wang, S. Z. Li, X. W. Dong, Z. B. Yan, H. L. Cai, and J.-M. Liu[a)]
Laboratory of Solid State Microstructures, Nanjing University, Nanjing 210093, China and International Center for Materials Physics, Chinese Academy of Sciences, Shenyang 110016, China

(Received 17 March 2009; accepted 4 April 2009; published online 28 April 2009)

Polycrystalline $CuCr_{1-x}Ni_xO_2$ is synthesized and its multiferrocity is characterized in order to enhance the ferromagnetism and ferroelectricity of $CuCrO_2$-based multiferroics. At the optimized doping level $x=0.05$, we observe not only an enhancement of one order of magnitude in magnetization but also a remarkable increasing of polarization up to $\sim 50\ \mu C/m^2$ from $\sim 35\ \mu C/m^2$ of polycrystalline $CuCrO_2$. It is argued that the Ni-doping may modulate the antiferromagnetic interactions between Cr^{3+} ions and probably induce the conical-like spin component responsible for the enhanced ferromagnetism. © *2009 American Institute of Physics*. [DOI: 10.1063/1.3125258]

In the past several years, special attention to multiferroics with coexisting ferroelectricity and magnetism as well as magnetoelectric (ME) coupling between them has been paid due to the promising potentials of applications.[1–5] While in early time the ME effects in Cr_2O_3 and $GdFeO_3$ (Refs. 6 and 7) etc were investigated, consequently barium fluorides $BaMF_4$ (where M is Mn, Fe, Co, or Ni) were found or predicted to exhibit high ferroelectric transition temperature and large polarization, thus attracting considerable interest.[8–11] More recently, multiferroics such as $HoMnO_3$ (Ref. 12) and $Ba_2CoGe_2O_7$ (Ref. 13) were synthesized and they belong to a class of materials known as "frustrated magnets," in which polarization originates from the spiral spin order due to the superspin current mechanism or the inverse Dzyaloshinskii–Moriya (DM) interaction,[14,15] although this mechanism may not be unique.

Those two-dimensional (2D) triangular antiferromagnets such as $CuFeO_2$[16] and $CuCrO_2$[17,18] attract attention too, since the ferroelectricity may be generated through a variation in the metal–ligand hybridization with spin–orbit coupling and thus can be modulated by the spin chirality.[19] For $CuCrO_2$, polarization P is activated associated with two successive magnetic transitions, first into a collinear antiferromagnetic (AFM) order and then an out-of-plane 120° spin ordering at temperature $T\sim 24$ K. So far, the measured P for polycrystalline CCO is $\sim 30\ \mu C/m^2$ (Ref. 20) and $\sim 90\ \mu C/m^2$ for single crystals parallel to the ab plane,[21] while the measured M is almost zero.

To modulate the spin chirality and then to enhance M and P in CCO, two roadmaps can be utilized. One is doping at Cr^{3+} sites by strong magnetic ions such as Fe^{3+} and Mn^{3+}, and the other is the doping by magnetic species of slightly different size. While Fe^{3+} and Mn^{3+} are much larger than Cr^{3+} ($r_i=0.645$, 0.645, and 0.615 Å for $i=Fe^{3+}$, Mn^{3+}, and Cr^{3+}), we adopt the second roadmap because such a substitution would only induce slight lattice distortion but modulate the AFM order of Cr^{3+} ions, which may help to tune the spin chirality and to develop other spin orders benefiting to enhanced M and P. On this basis, we choose Ni^{3+} ($r=0.60$ Å) to substitute Cr^{3+}.

In our experiment, we prepared a series of high quality polycrystalline $CuCr_{1-x}Ni_xO_2$ (CCNO) samples by solid state reaction. The crystallinity and microstructure of the samples were checked by X-ray diffraction (XRD) using Cu target, and the covalence state of the ions was checked by X-ray photoelectron spectroscopy (XPS) (PHI-550). The magnetization M was measured using the Quantum Design superconducting quantum interference device. The ferroelectricity was probed using the pyroelectric current method (using Keithley 6514), integrated with the Quantum Design Physical Properties Measurement System, where the dielectric data were collected using an impedance analyzer (HP 4294A). For probing P, each sample under a poling electric field $E\sim 430$ kV/m and various magnetic field H (0–9 T) was first cooled down to $T=2$ K, followed by a sufficiently long time short-circuit procedure. To obtain the T (H)-dependence of P, the pyroelectric current was collected at a 4 K/min T-sweeping rate (0.6 T/min H-sweeping rate) if any.

Figure 1(a) shows the XRD θ-2θ spectra of two samples at room temperature: one is CCO, and the other is $CuCr_{1-x}Ni_xO_2$ with $x=0.05$. All reflections can be assigned to the single delafossite rhombohedral structure with space group R-3m and no detectable impurity phase is available. For identifying possible structural distortion, we perform high-precision Rietveld refining of the XRD data, as shown in Figs. 1(b) and 1(c), for CCO and CCNO. A very small difference between the measured spectra and refined ones is shown. The reliability of the Rietveld refinement is demonstrated by the refinement parameters $R_{wp}=11.51\%$ with lattice parameters $a=2.977\ 66(5)$ Å and $c=17.099\ 80(23)$ Å for CCO, and $R_{wp}=10.72\%$ with $a=2.975\ 18(4)$ Å and $c=17.096\ 54(23)$ Å for CCNO. A slight contraction of both a and c due to the substitution is shown.

We performed multiferroic characterization of CCNO with various x. It seems that the doping of $x=0.05$ shows the optimized property in terms of P and M, and thus the data presented below refer to this doping level. The measured magnetic properties of both CCNO and CCO are summarized in Fig. 2. Figure 2(a) shows the field-cooling (FC) M as a function of T (cooling field $H=500$ Oe). Obviously the measured M for CCNO over the whole T-range (2–300 K) is 10–20 times larger than that for CCO, demonstrating a significantly enhanced ferromagnetism with respect to CCO.

a)Author to whom correspondence should be addressed. Electronic mail: liujm@nju.edu.cn.

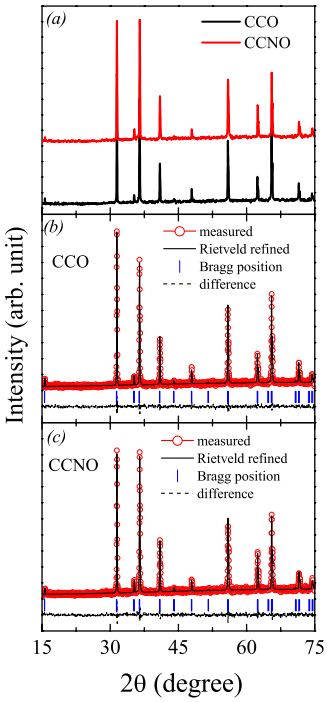

FIG. 1. (Color online) (a) XRD θ-2θ spectra for CCO and CCNO samples (open circle dot, measured, and solid line, using Rietveld structural refinement), respectively. The difference (dashed line, difference) between the measured and Rietveld refined spectra for the two samples, respectively, is plotted with a slight downshift for clarity in (b) and (c). The short vertical solid lines are guides for the eyes for the corresponding Bragg position.

Going into the details, we performed the FC and zero-field cooled (ZFC) measurements and the data are shown in Fig. 2(b). A clear irreversibility between the ZFC and FC curves is shown and the splitting ensues at $T \sim 250$ K and spreads over the whole T-range. This phenomenon allows us to argue the strong AFM background evidenced by the ZFC M-T curve and a spin-glasslike behavior. Although this behavior

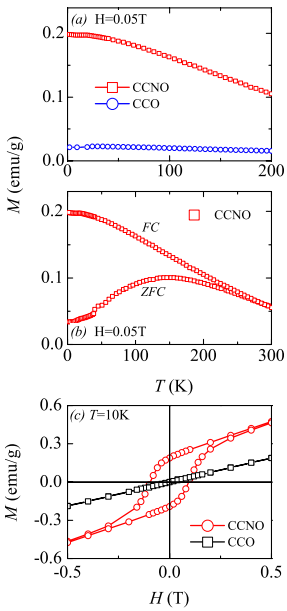

FIG. 2. (Color online) Measured M-T relation under (a) FC conditions for CCO and CCNO and (b) ZFC and FC conditions for CCNO with a magnetic field of 500 Oe. (c) Measured M-H hysteresis at 10 K for CCO and CCNO samples, respectively.

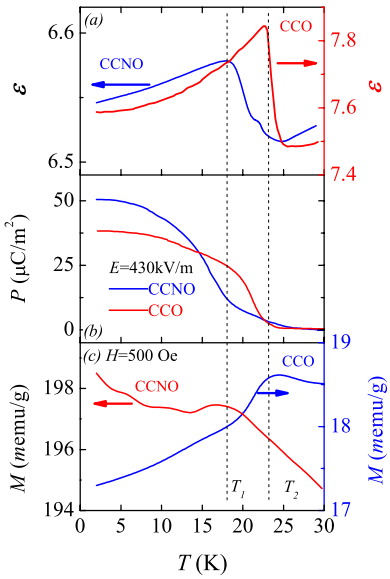

FIG. 3. (Color online) Temperature dependence of (a) dielectric constant ε and (b) electric polarization P under $H=0$ for CCO and CCNO, and magnetization M for (c) CCO and (d) CCNO.

is interesting, more investigations on its essence are necessary. In fact, similar behavior was observed for $BiFeO_3$.[22,23]

An additional fact is that CCNO does exhibit significant magnetization response to external magnetic field. To further reveal this point, we present the measured M-H hysteresis at $T=10$ K for both CCNO and CCO, as shown in Fig. 2(c). While no loop for CCO is shown, a remarkable loop for CCNO is observed, giving rise to a coercivity of ~ 1000 Oe and remnant magnetization of ~ 0.25 emu/g, although no magnetization saturation is obtained, probably due to the spin-glasslike essence. Therefore, the substantial ferromagnetic component in the magnetism of CCNO is revealed.

Given the enhanced ferromagnetism, we need to check the ferroelectricity of CCNO. The measured dielectric constant ε and P for both CCO and CCNO are shown in Figs. 3(a) and 3(b). It is seen that CCNO and CCO show clear dielectric peaks at $T \sim 18$ and ~ 23 K, respectively, corresponding to the ferroelectric transitions, noting that the peak of CCO is consistent with an earlier report.[20] These transitions are further evidenced by the measured P in Fig. 3(b). Although the transition point of CCNO is slightly lower than that of CCO, the low-T polarization P (~ 50 $\mu C/m^2$) of CCNO is even larger than that of CCO (~ 35 $\mu C/m^2$), indicating that the Ni-doping does not damage the ferroelectricity of CCO but even enhances it simultaneously with the enhanced ferromagnetism.

The next issue is the ME coupling between the ferroelectricity and magnetism. First, small anomalies of M in response to the ferroelectric transitions at $T \sim 23$ K, is observed, as shown in Fig. 3(c), for CCO. This anomaly can be identified as an AFM ordering. For CCNO, it was observed that the anomaly is shoulderlike, appearing at $T \sim 18$ K where P increases rapidly with decreasing T, although small polarization is identifiable slightly above ~ 18 up to ~ 23 K. This anomaly seems also to be an indication of an AFM ordering. These anomalies are clear indications of the ME coupling, and the underlying physics is straightforward by considering the fact that the AFM order with the proper spin

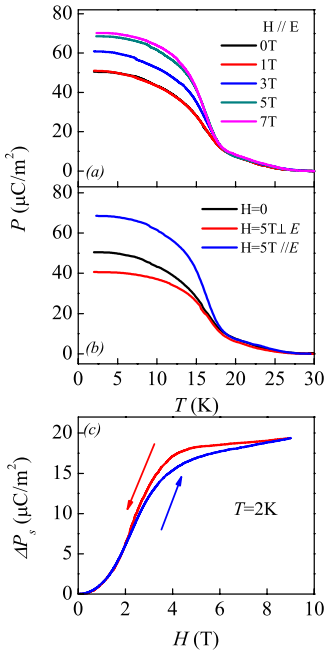

FIG. 4. (Color online) (a) Temperature dependence of electric polarization P in the selected magnetic field for CCNO, (b) magnetic field dependence of electric polarization at $T=2$ K, and (c) variation in electric polarization P with temperature in $H=0$, $H=5$ T$\|E$, and $H=5$ T$\perp E$.

chirality can be further stabilized by the established ferroelectric order via their coupling.

Additional evidence with the ME coupling in CCNO is given by the response of P to H applied in two types of geometry, as shown in Fig. 4. Figure 4(a) plots P as a function of T under various H in parallel to electric field E. It is seen that H enhances significantly the low-T polarization while no impact on the ferroelectric transition point is observed. Such an effect becomes saturated at $H>5$ T. On the other hand, a magnetic field in perpendicular to E suppresses the polarization, as shown in Fig. 4(b). These results demonstrate convincingly the strong ME coupling and furthermore its anisotropy. To elucidate P as a function of H, we present in Fig. 4(c) the isothermal curve of ΔP against varying H (0–9 T) in a cycle at $T=2$ K. It is seen that P is insensitive to H in the low-H range ($H<\sim 0.4$ T), but sharply increases in the intermediate H (~ 1 T$<H<\sim 5$ T) before saturated above $H\sim 5$ T.

To understand the effect of the Ni doping, we consider Cr^{3+} spin configuration in CCO. Our XPS data identified no valence state other than Cr^{3+} and Cu^{1+} in CCNO, indicating the existence of Ni^{3+} ions. On the other hand, Ni^{2+} doping ($r=0.69$ Å) must make expansion of the lattice which does not occur here. The Ni-doping induced weak ferromagnetism may be attributed to a conical spin magnetic structure, allowing a tuning of P by H.[24] This possibility was recently revealed[25] and a proper screw type of magnetic order can induce ferroelectricity through the spin-orbit interaction bringing some modification on the d-p hybridization between ligand and $3d$ magnetic ions, which was used to explain the origin of polarization in $CuFe_{1-x}Al_xO_2$ (Refs. 19 and 26) and is argued to apply to CCNO here. On the other hand, it was proposed that ferroelectricity can also induce weak ferromagnetism (and vice versa) by a ME coupling via the DM interaction in a low-symmetry ferroelectric system,[27,28] which may also contribute to the weak ferromagnetism in the present CCNO.

For the response of P to H, we consult to the microscopic origin of P in CCO.[21] Given the sixfold symmetry on the triangular lattice plane and taking also into account of the triply degenerated 120° spin structure as well as the doubly degenerated spin chirality, there exist six types of magnetic domains. Assuming the one-to-one correspondence between the signs of P and the spin chirality, there should exist six types of spin-chiral ferroelectric domains.

For $H\|E$, the domains with the spiral plane parallel to E is stabilized, that is, the ferroelectric domains with $P\|H$ becomes more stable than others, leading other domains to rotate toward the direction of E and thus explaining the enhanced P upon increasing H, as displayed in Fig. 4(b). However, these domains become unstable if $H\perp E$. Therefore, for $H\perp E$, polarization P of the lattice as a whole will be reduced, as shown in Fig. 4(b).

This work was supported by the Natural Science Foundation of China (Grant Nos. 50601013 and 50832002), the National Key Projects for Basic Research of China (Grant Nos. 2009CB623303 and 2009CB929501), and the 111 Programme of MOE of China (Grant No. B07026).

[1] M. Fiebig, J. Phys. D: Appl. Phys. **38**, R123 (2005).
[2] S. W. Cheong and M. Mostovoy, Nature Mater. **6**, 13 (2007).
[3] R. Ramesh and N. A. Spaldin, Nature Mater. **6**, 21 (2007).
[4] J. F. Scott, Nature Mater. **6**, 256 (2007).
[5] Y. Tokura, J. Magn. Magn. Mater. **310**, 1145 (2007).
[6] I. E. Dzyaloshinskii, Sov. Phys. JETP **10**, 628 (1959).
[7] G. T. Rado, Phys. Rev. Lett. **13**, 335 (1964).
[8] J. F. Scott, Phys. Rev. B **16**, 2329 (1977).
[9] G. A. Samara and P. M. Richards, Phys. Rev. B **14**, 5073 (1976).
[10] J. F. Scott, Rep. Prog. Phys. **42**, 1055 (1979).
[11] C. Ederer and N. A. Spaldin, Phys. Rev. B **74**, 024102 (2006).
[12] Th. Lottermoser, T. Lonkai, U. Amann, D. Hohlwein, J. Ihringer, and M. Fiebig, Nature (London) **430**, 541 (2004).
[13] H. T. Yi, Y. J. Choi, S. Lee, and S.-W. Cheong, Appl. Phys. Lett. **92**, 212904 (2008).
[14] I. A. Sergienko and E. Dagotto, Phys. Rev. B **73**, 094434 (2006).
[15] Q. Li, S. Dong, and J.-M. Liu, Phys. Rev. B **77**, 054442 (2008).
[16] T. Kimura, J. C. Lashley, and A. P. Ramirez, Phys. Rev. B **73**, 220401(R) (2006).
[17] H. Kadowaki, H. Kikuchi, and Y. Ajiro, J. Phys.: Condens. Matter **2**, 4485 (1990).
[18] M. F. Collins and O. A. Petrenko, Can. J. Phys. **75**, 605 (1997).
[19] T. Arima, J. Phys. Soc. Jpn. **76**, 073702 (2007).
[20] S. Seki, Y. Onose, and Y. Tokura, Phys. Rev. Lett. **101**, 067204 (2008).
[21] K. Kimura, H. Nakamura, K. Ohgushi, and T. Kimura, Phys. Rev. B **78**, 140401(R) (2008).
[22] M. K. Singh, W. Prellier, M. P. Singh, R. S. Katiyar, and J. F. Scott, Phys. Rev. B **77**, 144403 (2008).
[23] M. K. Singh, R. S. Katiyar, W. Prellier, and J. F. Scott, J. Phys.: Condens. Matter **21**, 042202 (2009).
[24] Y. Yamasaki, S. Miyasaka, Y. Kaneko, J.-P. He, T. Arima, and Y. Tokura, Phys. Rev. Lett. **96**, 207204 (2006).
[25] C. Jia, S. Onoda, N. Nagaosa, and J. H. Han, Phys. Rev. B **74**, 224444 (2006).
[26] T. Nakajima, S. Mitsuda, S. Kanetsuki, K. Tanaka, and K. Fujii, Phys. Rev. B **77**, 052401 (2008).
[27] D. L. Fox and J. F. Scott, J. Phys. C **10**, L329 (1977).
[28] D. L. Fox, D. R. Tilley, J. F. Scott, and H. J. Guggenheim, Phys. Rev. B **21**, 2926 (1980).